Single *d*(GpG)/*cis*-Diammineplatinum(II) Adduct-Induced Inhibition of DNA Polymerization

Zucai Suo,[§,||] Stephen J. Lippard,[⊥] and Kenneth A. Johnson*[,§,¶]

Department of Biochemistry and Molecular Biology, 106 Althouse Laboratory, The Pennsylvania State University, University Park, Pennsylvania 16802, and Department of Chemistry, Massachusetts Institute of Technology, Cambridge, Massachusetts 02139

Received August 3, 1998; Revised Manuscript Received October 30, 1998

ABSTRACT: A 44 nucleotide DNA template containing a single site-specifically placed cisplatin adduct (*cis*-[Pt(NH$_3$)$_2$\{d(GpG)-N7(1),-N7(2)\}]) was annealed with a primer, positioning its 3′-end four bases before the adduct in the template strand. DNA polymerization in the presence of all four nucleotides revealed that both HIV-1 reverse transcriptase (RT) and T7 DNA polymerase strongly paused at one nucleotide preceding the first platinated guanine and at the positions opposite the two platinated guanines. Analysis of single nucleotide incorporation at each pause site showed that polymerization occurs with biphasic kinetics. A small percentage of DNA was bound productively, providing a small amplitude (1−3%) of a fast phase of polymerization, whereas most of the bound DNA (1−34%) was positioned at the pause site in a nonproductive manner and therefore elongated slowly (0.04−0.06 s^{-1}). DNA substrates annealed to the cisplatin-modified template bind to HIV-1 RT with an affinity (10−20 nM) similar to that of unmodified substrates (6−9 nM). The cisplatin−DNA cross-link moderately weakened DNA binding to T7 DNA polymerase (12−115 nM) but significantly slowed the rate of incorporation of the next nucleotide (2−7 s^{-1}), with larger effects closer to the cisplatin−DNA adduct. The crystal structure of the same cisplatin−DNA adduct [Takahara, P. M., Frederick, C. A., and Lippard, S. J. (1996) *J. Am. Chem. Soc. 118*, 12309−12321] reveals not only the bent DNA duplex but also the propeller twisted base pairs near the cisplatin−DNA adduct. The twisted base pairs may cause misalignment of the cisplatin-modified DNA at the binding cleft of T7 DNA polymerase and significantly slow the rate of the protein conformational change preceding polymerization, leading to the slight accumulation of intermediates within five base pairs of the adduct. The ground-state binding of the next correct nucleotide to the enzyme•DNA complex was weakened by the adduct with T7 DNA polymerase but unchanged with HIV-1 RT at sites other than the three strong pause sites. Nucleotide binding to both enzymes at the three strong pause sites was significantly weaker and less selective.

The widely used antitumor drug *cis*-diamminedichloroplatinum(II) (cisplatin)[1] targets cellular DNA forming thousands of intra- and interstrand bifunctional covalent adducts with the bases (*1*, *2*). The most abundant DNA adducts formed by cisplatin are *cis*-[Pt(NH$_3$)$_2$\{d(GpG)-N7(1),-N7(2)\}] (65%) and *cis*-[Pt(NH$_3$)$_2$\{d(ApG)-N7(1),-N7(2)\}] (25%) intrastrand cross-links (*1*); interstrand cross-links comprise only 5% of the adducts (*3*). The antitumor activity of cisplatin is thought to be related to the formation of intrastrand DNA adducts (*4*, *5*). Biochemical studies have revealed that the platinum−DNA covalent adducts inhibit replication (*3*), transcription (*6*), and DNA repair (*7*, *8*). With DNA templates containing site-specifically-placed platinum−DNA adducts, several DNA polymerases with varied function, fidelity, and processivity were severely blocked but could traverse through all of the major cisplatin−DNA adducts (*3*). In this report, we examine the effects of a site-specific cisplatin adduct on DNA polymerization using single turnover kinetic methods.

The binding of cisplatin to DNA not only leads to significant biological consequences but also dramatically alters the structure of the double helix. This structural distortion has been clearly shown by the crystallographic determination of a DNA dodecamer duplex containing a single *cis*-[Pt(NH$_3$)$_2$\{d(GpG)-N7(1),-N7(2)\}] cross-link (*9*, *10*) and by several NMR studies (*11*−*13*). The structural work reveals that cisplatin bends the duplex by 39−55° in the crystal (*9*) and by 78° in solution (*13*) at the site of the two modified guanines (center bases), widens the minor groove (*13*), distorts base pairs (*13*), and alters the B-type

[†] This work was supported by National Institutes of Health Grants GM44613 to K.A.J. and CA34992 to S.J.L.

* To whom correspondence should be addressed.

[§] The Pennsylvania State University.

[||] Current address: Department of Biological Chemistry and Molecular Pharmacology, Harvard Medical School, Boston, MA 02115.

[⊥] Massachusetts Institute of Technology.

[¶] Current address: Institute for Cellular and Molecular Biology, 2500 Speedway, University of Texas at Austin, Austin, TX 78712. Telephone: (512) 471-0434. Fax: (512) 471-0435. E-mail: kaj1@psu.edu.

[1] Abbreviations: AIDS, acquired immunodeficiency syndrome; BSA, bovine serum albumin; cisplatin, *cis*-diamminedichloroplatinum(II); DTT, dithiothreitol; d4T, 3′-deoxy-2′,3′-didehydrothymidine; dNTP, deoxynucleoside triphosphate; EDTA, ethylenediaminetetraacetic acid; HIV, human immunodeficiency virus; RT, reverse transcriptase; T7 exo$^-$, an exonuclease-deficient T7 DNA polymerase with the D3A and E7A double-point mutations; TBE, 89 mM TRIS, 89 mM borate, and 2 mM EDTA.

10.1021/bi981854n CCC: $18.00
Published on Web 12/19/1998

DNA to an A-type geometry (*9*). Surprisingly, the geometrical change of the DNA containing a single *cis*-[Pt(NH$_3$)$_2$\{d(GpG)-N7(1),-N7(2)\}] cross-link is similar to that of DNA bound by HIV-1 RT (*14*) or T7 DNA polymerase (*15*), as described below. Thus, cisplatin-modified DNA affords an interesting model substrate for evaluating the effect of DNA bending on the polymerase activities of HIV-1 RT and T7 DNA polymerase.

Reverse transcriptase (RT) from the human immunodeficiency virus type 1 (HIV-1) copies single-stranded viral genomic RNA into double-stranded DNA prior to integration into host cell chromosomes (*16*). HIV-1 RT possesses RNA template-dependent DNA polymerase activity, DNA template-dependent DNA polymerase activity, and RNase H activity (*17*). HIV-1 RT has relatively low processivity and fidelity (*18*) for an enzyme involved in replication. The mechanism of polymerization catalyzed by HIV-1 RT has been elucidated by pre-steady-state kinetic methods (*19*−*22*). The crystal structure of HIV-1 RT complexed with a DNA 18/19-mer duplex (RT·DNA) has been reported (*14*), as have the structures of unliganded HIV-1 RT (*23*) and of HIV-1 RT complexed with a nonnucleoside inhibitor Nevirapine (*24*). The crystal structure of the RT·DNA complex revealed the duplex to have an unusual and unexpected bend at the active site (*14*). The majority of the 18 base pair duplex region is B-type, but in the vicinity of the polymerase active site there are about 4 base pairs of DNA which are A-type, and at the junction between the A-type and B-type regions of the 18/19-mer there is a marked bend (40−45°). Such a structural distortion may alter the RT functions of catalysis, translocation, fidelity, and processivity (*14*).

T7 DNA polymerase (*25*) replicates T7 phage DNA with high fidelity and processivity. It has both 5′−3′ DNA polymerase activity and 3′−5′ exonuclease proofreading activities. The mechanism of polymerization catalyzed by T7 DNA polymerase has also been elucidated by pre-steady-state kinetic methods (*26*−*28*). Recently, the crystal structure of T7 DNA polymerase complexed with *Escherichia coli* (*E. coli*) thioredoxin, a DNA 22/26-mer duplex, and the next correct nucleotide has been solved at 2.2 Å resolution (*15*). This crystal structure revealed that the DNA was doubly bent to produce an S-shape through extensive interactions with T7 DNA polymerase near the polymerase active site. The two base pairs at the primer 3′-end are A-form, and the rest of the DNA is in B-form. The effect of DNA bending on polymerase activity is not understood.

In the present paper, we have constructed a 44 nucleotide template containing a site-specifically-placed *cis*-[Pt(NH$_3$)$_2$\{d(GpG)-N7(1),-N7(2)\}] intrastrand cross-link to assess the effect of DNA bending on the polymerase activities of HIV-1 RT and T7 DNA polymerase. By using transient kinetic methods, we discovered that both enzymes strongly paused during DNA synthesis at one nucleotide preceding the first platinated guanine and at the positions opposite the two platinated guanines. The mechanistic basis of polymerization pausing due to *cis*-[Pt(NH$_3$)$_2$\{d(GpG)-N7(1),-N7(2)\}] cross-link is described.

MATERIALS AND METHODS

Proteins. Wild-type HIV-1 RT was overexpressed and purified as described (*29*). The exonuclease-deficient mutant (D5A and E7A) of T7 DNA polymerase (T7 exo$^-$) was prepared according to a published procedure (*26*). *E. coli* thioredoxin was purchased from Promega and combined with the T7 polymerase to form the holoenzyme used in all experiments. The protein concentrations were determined spectrophotometrically at 280 nm, using the extinction coefficients of 260 450 (HIV-1 RT), 144 000 (T7 exo$^-$), and 13 700 (*E. coli* thioredoxin) M^{-1} cm^{-1}.

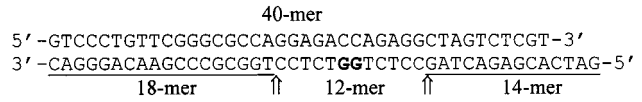

FIGURE 1: Synthesis of 44-cisplatin. The arrows denote the site of ligation of individual oligomers. The bottom oligomers 14- and 18-mer are underlined. The two cisplatin-modified guanines of 12-mer are in boldface. The ligation template is the top oligomer 40-mer. These four oligomers were mixed, annealed, and ligated as described in Materials and Methods.

Materials. [γ-^{32}P]ATP was purchased from ICN. dNTPs were obtained from Pharmacia. Biospin columns were purchased from Bio-Rad.

Synthetic Oligonucleotides. To construct the cisplatin-modified 44 nucleotide DNA template, a DNA 12-mer containing a single *cis*-[Pt(NH$_3$)$_2$\{d(GpG)-N7(1),-N7(2)\}] intrastrand cross-link (*9*), prepared as described previously (*30*), was ligated with two other purified oligomers, an 18-mer and a 14-mer (Figure 1). First, the DNA 12-mer and 18-mer were 5′-phosphorylated by using T4 polynucleotide kinase (New England Biolabs). Then, the 5′-phosphorylated 12-mer and 18-mer were annealed with nonphosphorylated DNA 40-mer and 14-mer at the molar ratio of 1.0:1.0:1.0:1.0 to form the DNA complex of 40-mer/14-12-18-mer (Figure 1). Finally, T4 ligase buffer and T4 DNA ligase (New England Biolabs) were added to the annealing mixture according to the manufacturer's protocol, to start the ligation. The ligation was performed at 16 °C for 12 h; then additional ligase and ligase buffer were added and incubated for another 12 h. The ligated 44-mer containing a single *cis*-[Pt(NH$_3$)$_2$\{d(GpG)-N7(1),-N7(2)\}] cross-link (44-cisplatin, Table 1) was purified by electrophoresis through 10% acrylamide/8 M urea and 1 × TBE (89 mM Tris, 89 mM borate, 2 mM EDTA). The purified DNA 44-cisplatin was 5′ ^{32}P-labeled, electrophoresed on a sequencing gel, and autoradiographed to determine purity. The 44-cisplatin migrates more slowly than the unmodified control 44-mer (44-control, Table 1). The concentration of the purified 44-cisplatin was measured spectrophotometrically at 260 nm, using an extinction coefficient of 457 480 M^{-1} cm^{-1} (*31*).

The 14-, 18-, and 40-mer oligomers (Figure 1), 44-control, and DNA primers listed in Table 1 which are complementary to the 3′ termini of the DNA 44-mer were synthesized on an Oligo 1000 DNA synthesizer (Beckman). All DNA oligomers were purified by denaturing polyacrylamide gel electrophoresis (20% acrylamide, 8 M urea), and their concentrations were determined by UV absorbance at 260 nm. Before annealing, DNA primers were 5′ ^{32}P-labeled with T4 polynucleotide kinase (New England Biolabs) according to manufacturer's instructions. Unincorporated nucleotide was removed by using a Biospin-30 column (Bio-Rad).

The DNA substrates were formed by annealing primers and templates at a molar ratio of 1.0:1.0. Prior to annealing,

Table 1: DNA Primers and Templates[a]

19-mer	5′-GTCCCTGTTCGGGCGCCAG-3′
22-mer	5′-GTCCCTGTTCGGGCGCCAGGAG-3′
23-mer	5′-GTCCCTGTTCGGGCGCCAGGAGA-3′
24-mer	5′-GTCCCTGTTCGGGCGCCAGGAGAC-3′
25-mer	5′-GTCCCTGTTCGGGCGCCAGGAGACC-3′
26-mer	5′-GTCCCTGTTCGGGCGCCAGGAGACCA-3′
27-mer	5′-GTCCCTGTTCGGGCGCCAGGAGACCAG-3′
28-mer	5′-GTCCCTGTTCGGGCGCCAGGAGACCAGA-3′
29-mer	5′-GTCCCTGTTCGGGCGCCAGGAGACCAGAG-3′
30-mer	5′-GTCCCTGTTCGGGCGCCAGGAGACCAGAGG-3′
31-mer	5′-GTCCCTGTTCGGGCGCCAGGAGACCAGAGGC-3′
32-mer	5′-GTCCCTGTTCGGGCGCCAGGAGACCAGAGGCT-3′
44-cisplatin	3′-CAGGGACAAGCCCGCGGTCCTCT**GG**TCTCCGATCAGAGCACTAG-5′
44-control	3′-CAGGGACAAGCCCGCGGTCCTCTGGTCTCCGATCAGAGCACTAG-5′

[a] The cisplatin-modified guanines are in boldface.

mixtures were denatured at 85 °C for 5 min and then cooled slowly to room temperature for 2 h. The DNA trap 25-/45-mer duplex described previously (*19*) was prepared similarly.

Buffers. All experiments using HIV-1 RT were performed in a buffer containing 50 mM Tris acetate (pH 7.5 at 37 °C), 10 mM magnesium acetate, 100 mM potassium acetate, and 0.1 mM EDTA. T7 exo$^-$ was preincubated with DNA substrate, *E. coli* thioredoxin, and DTT in T7 buffer containing 40 mM Tris chloride (pH 7.5 at 20 °C), 50 mM sodium chloride, 1 mM EDTA, 1 mM DTT, and 0.1 mg/mL BSA as described (*26*). All reactions using T7 exo$^-$ were carried out at 20 °C in the T7 buffer containing 12.5 mM magnesium chloride.

Rapid-Quench Experiments. Experiments were carried out in a rapid chemical quench flow apparatus designed by Johnson (*32*) and built by KinTek Corp. (Austin, TX, www.kintek-corp.com). The apparatus contained a computer-controlled stepping motor and was modified for small reaction volumes (15 μL). The experiments were typically carried out by loading the enzyme solution in one loop (15 μL) and the substrate solution in the second loop (15 μL) of tubing. The solutions were rapidly mixed and quenched with 0.3 M EDTA (final concentration) after time intervals ranging from 5 ms to several minutes. Unless noted otherwise, all concentrations are those after mixing.

Pre-Steady-State Kinetic Analysis for Incorporation of Next Correct Nucleotide. This analysis was conducted under conditions where the DNA was in slight excess over the enzyme concentration. The reactions were performed by mixing a solution containing the preincubated complex of 60 nM HIV-1 RT or T7 exo$^-$ and 5′-labeled 200 nM DNA with a solution of 100 μM Mg^{2+}·dNTP at the appropriate reaction temperature. Polymerization was quenched with 0.3 M EDTA at time intervals ranging from 5 ms to 7 s. DNA products were quantitated by sequencing gel analysis.

Nitrocellulose−DEAE Membrane Double-Filter Binding Assay. This procedure was described previously (*29*, *33*). Filter binding was carried out by using a 96-well dot-blot apparatus, nitrocellulose, and DEAE membranes from Schleicher & Schuell. This assay is based on the ability of the nitrocellulose membrane to retain RT·DNA and the DEAE membrane to trap all free DNA substrates.

Wild-type RT (60 nM) was preincubated with increasing concentrations of DNA duplex in binding buffer (50 mM Tris acetate, 10 mM magnesium acetate, 100 mM potassium acetate, 0.1 mM EDTA, pH 7.5 at 23 °C). Immediately prior to filtering each sample, the well was washed with 100 μL of binding buffer. With a vacuum applied, 20 μL of each sample was added to the well followed by 100 μL of buffer, and the procedure was repeated twice for each DNA concentration. Following titration, substrate binding was quantitated by using a 445 SI Phosphorimager (Molecular Dynamics, Sunnyvale, CA).

Product Analysis. Reaction products were analyzed by sequencing gel electrophoresis (10−16% acrylamide, 8 M urea, 1 × TBE running buffer) and quantitated with a 445 SI Phosphorimager.

Data Analysis. Data were fitted by nonlinear regression using a program GraFit (Erithacus Software). Data from burst experiments were fitted to eq 1, where A is the fraction of

$$[\text{Product}] = AE_0[1 - \exp(-k_1 t) + k_2 t] \quad (1)$$

active enzyme, E_0 the enzyme concentration measured spectrophotometrically, k_1 the observed burst rate, and k_2 the observed steady-state rate. The biphasic kinetic data were fitted to eq 2, where E_0 represents the total enzyme

$$[\text{Product}] = E_0A_1[1 - \exp(-k_1 t)] + E_0A_2[1 - \exp(-k_2 t)] \quad (2)$$

concentration measured spectrophotometrically, A_1 the fast-phase enzyme amplitude, k_1 the observed fast-phase rate, A_2 the fast-phase enzyme amplitude, and k_2 the observed slow phase rate. The single-phase kinetic data were fitted to eq 3,

$$[\text{Product}] = E_0A[1 - \exp(-kt)] \quad (3)$$

where E_0 represents the enzyme concentration measured spectrophotometrically, A the enzyme amplitude, and k the observed rate. Data from measurement of K_d of dNTP were fitted to eq 4, where k_p is the maximum rate of dNTP

$$k_{obs} = k_p[\text{dNTP}]/\{[\text{dNTP}] + K_d\} \quad (4)$$

incorporation. Data from the active site titration and nitrocellulose−DEAE double-filter binding assay were fitted to eq 5, where K_d represents the equilibrium dissociation constant

$$[\text{E·DNA}] = 0.5(K_d + E_0 + D_0) - 0.5[(K_d + E_0 + D_0)^2 - 4E_0D_0]^{1/2} \quad (5)$$

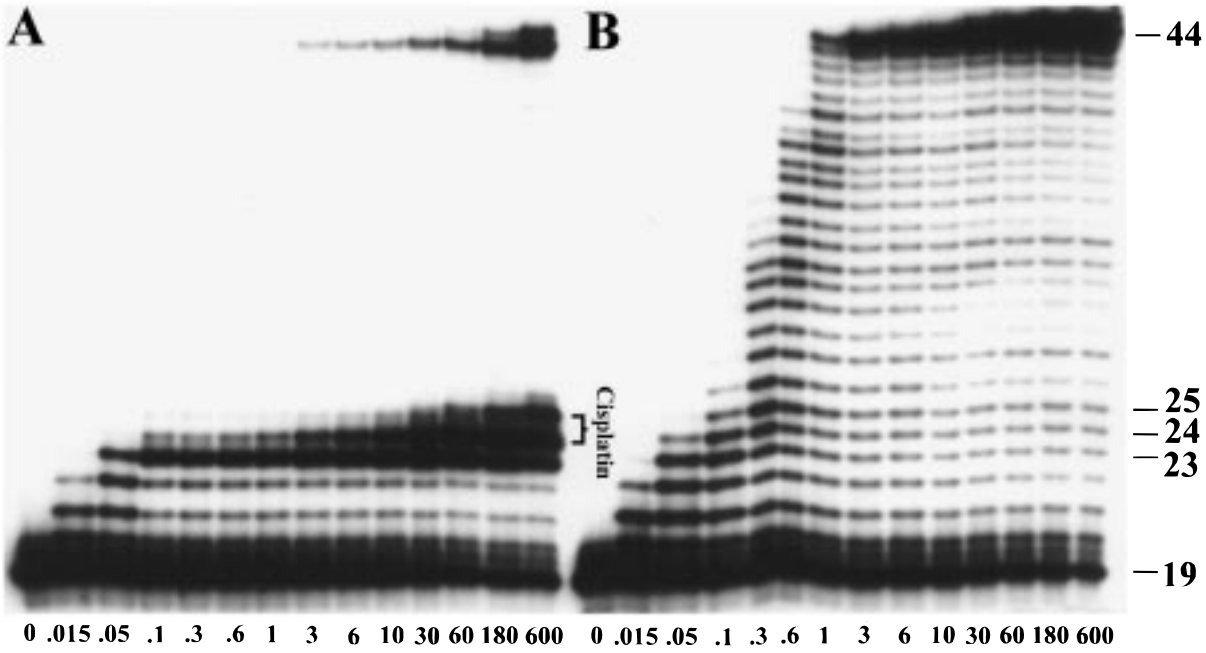

FIGURE 2: Processive polymerization catalyzed by wild-type HIV-1 RT at 37 °C. A preincubated solution of HIV-1 RT (100 nM) and 5′ ^{32}P-labeled 19/44-mer (100 nM) in RT buffer was mixed with dNTPs (150 μM each) and magnesium acetate (10 mM) (final concentrations) in RT buffer (pH 7.5) at 37 °C. The reactions were quenched with 0.3 M EDTA at the indicated times and analyzed by sequencing gel electrophoresis: (A) the 19/44-cisplatin (the two strong pause sites opposite the cisplatin-modified guanines were marked "cisplatin"); (B) the 19/44-control.

for DNA substrates, E_0 the active enzyme concentration, and D_0 the DNA concentration.

RESULTS

Construction of a 44 Nucleotide DNA Template Containing a Site-Specifically-Placed cis-[Pt(NH$_3$)$_2$\{d(GpG)-N7(1),-N7(2)\}] Intrastrand Cross-Link. A DNA template based on the structurally characterized cisplatin-modified 12-mer duplex (*9*) was prepared by ligation to a 14-mer and an 18-mer. This procedure generated a 44 nucleotide template containing a single *cis*-[Pt(NH$_3$)$_2$\{d(GpG)-N7(1),-N7(2)\}] cross-link (44-cisplatin) (see Figure 1 and Materials and Methods). This synthetic strategy allowed us to include bases of G and A at several positions in the template in addition to the cisplatin-modified guanines. The first 18 nucleotides on the 3′ terminus of the 44-cisplatin DNA are derived from the sequence of the tRNA^{Lys,3} primer binding site of the HIV-1 RNA genome for HIV-1 replication initiation (*34*). The two modified guanines are located at the 24th and 25th positions from the 3′ terminus. After annealing a 19 nucleotide primer to the 3′ terminus of 44-cisplatin, we examined processive DNA polymerization through the single *cis*-[Pt(NH$_3$)$_2$\{d(GpG)-N7(1),-N7(2)\}] cross-link on the template. Polymerization to form primer extension products of 24 and 25 bases in length corresponds to the sites opposite the modified guanines in the template.

Processive Polymerization on the 19/44-Cisplatin and the 19/44-Control Substrates. Elongation of the 19/44-cisplatin primer/template duplex was tested by rapidly mixing a preincubated solution of HIV-1 RT, Mg^{2+}, and DNA with a solution containing all four nucleotides. The reaction was stopped at various times, and the products were analyzed using a sequencing gel, as shown in Figure 2A. In comparison, the same experiment performed with the unmodified control template 44-mer (44-control) afforded the results shown in Figure 2B. Polymerization using the 44-cisplatin template proceeded rapidly up to the nucleotide preceding and at the sites opposite the platinum atom, such that the 23, 24, and 25 nucleotide intermediates accumulated to a significant extent. There was almost no accumulation of larger DNA intermediates with the 44-cisplatin template, whereas all intermediate products were seen at lower levels with the 44-control template as the full-length product was being formed. A small amount of the full-length products accumulated with the 44-cisplatin template, but only at the longer reaction times. At even longer times, more full-length product was formed, indicating that the enzyme could read through the adduct given sufficient time.

To test whether the cisplatin adduct also causes pausing of the highly processive and selective enzyme T7 DNA polymerase, we performed similar experiments with both substrates using T7 exo$^-$ at 20 °C (Figure 3). With the 44-cisplatin template, T7 exo$^-$ strongly paused after the synthesis of the 23- and 24-mer. There was a small amount of the 25-mer and the full-length products even after a 10 min reaction; other intermediates are almost nondetectable, consistent with the overall higher fidelity of T7 DNA polymerase. With the 44-control template, there was no significant accumulation of intermediates and all elongation products were seen in approximately equal amounts.

Kinetics of Polymerization at Pause and Nonpause Sites. The accumulation of intermediates suggests that the kinetics

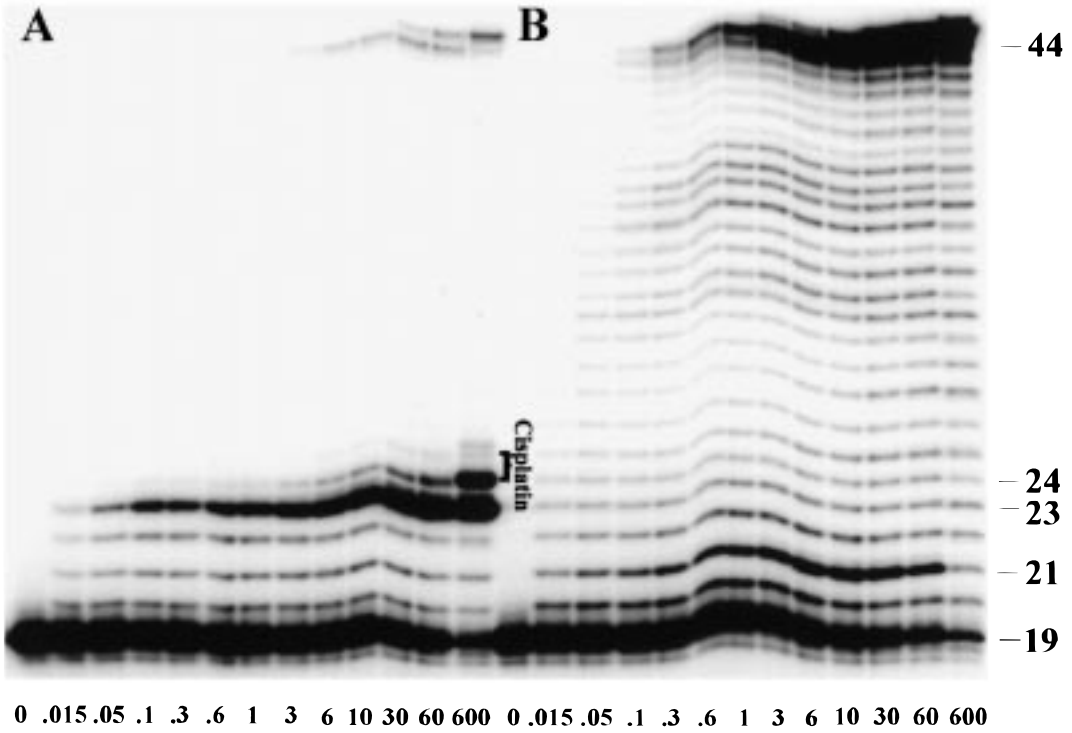

FIGURE 3: Processive polymerization catalyzed by the exonuclease-deficient T7 DNA polymerase at 20 °C. A preincubated solution of T7 DNA polymerase (100 nM), *E. coli* thioredoxin (2 μM), and 5′ ^{32}P-labeled 19/44-mer (100 nM) in T7 buffer was mixed with dNTPs (150 μM each) and magnesium chloride (12.5 mM) (final concentrations) in T7 buffer (pH 7.5) at 20 °C. The reactions were quenched with 0.3 M EDTA at the indicated times and analyzed by sequencing gel electrophoresis: (A) the 19/44-cisplatin (the two strong pause sites opposite the cisplatin-modified guanines were marked "cisplatin"); (B) the 19/44-control.

Table 2: Kinetic Constants and Binding Affinity of Wild-Type HIV-1 RT and DNA Substrates with the 44-Cisplatin Template at 37 °C[a]

substrate	fast rate (s^{-1})	amplitude (fast phase) (%)	slow rate (s^{-1})	amplitude (slow phase) (%)	$K_{d,DNA}$ (nM) polymerase site	$K_{d,DNA}$ (nM) overall
22/44-mer	19 ± 2	92 ± 2			27 ± 5	16 ± 3
23/44-mer	32 ± 17	2.8 ± 0.4	0.061 ± 0.004	22.0 ± 0.5	1663 ± 640	20 ± 2
24/44-mer	24 ± 4	1.1 ± 0.1	0.042 ± 0.009	1.1 ± 0.2	649 ± 251	18 ± 4
25/44-mer	27 ± 22	1.4 ± 0.4	0.041 ± 0.003	34 ± 1	489 ± 235	18 ± 3
26/44-mer	30 ± 3	50.7 ± 0.5			17 ± 2	18 ± 4
27/44-mer	38 ± 2	52.9 ± 0.7			16 ± 4	11 ± 3
30/44-mer	34 ± 2	51.3 ± 0.8			10 ± 3	10 ± 4

[a] The substrates corresponding to the strong pause sites are in boldface. All data except the overall DNA binding constants (23 °C) were obtained at 37 °C.

of polymerization catalyzed by RT and T7 exo$^-$ are significantly affected by the *cis*-[Pt(NH$_3$)$_2$\{d(GpG)-N7(1),-N7(2)\}] cross-link. To investigate the mechanistic basis for enzyme pausing, we performed a pre-steady-state kinetic analysis of single nucleotide incorporation at each pause site and at several nonpause sites as described in Materials and Methods. Primers of different length were synthesized as shown in Table 1, annealed to the 44-cisplatin or 44-control template, and used to examine the kinetics of a single nucleotide incorporation. This series of template primer duplexes allowed detailed analysis of the kinetics of polymerization at each pause site.

The time course of product formation catalyzed by HIV-1 RT at each nonpause site with the 44-cisplatin template, or at each site with the 44-control template, showed a "burst" phase followed by a slower steady-state phase (not shown). The primary data parallel those described previously (*19*). The rates of polymerization obtained by fitting the data to eq 1 (see Materials and Methods) are summarized in Table 2 with the 44-cisplatin template and in Table 3 with the 44-control template. For example, the incorporation of dATP into 27/44-cisplatin occurred at a rate of 38 s^{-1} and a reaction amplitude of 53% (relative to total enzyme concentration) in the burst phase followed by a steady-state phase at a rate of 0.05 s^{-1}. The fast burst phase of the reaction represents the rapid formation of product at the polymerase active site, while the steady-state phase is limited by the slow release of product from the enzyme. This behavior is typical of the reaction kinetics observed at all nonpause sites with the 44-cisplatin template and at all sites with the 44-control template. All measured steady-state rates (not listed) are in the range of 0.02−0.09 s^{-1}.

Table 3: Kinetic Constants and Binding Affinity of Wild-Type HIV-1 RT and DNA Substrates with the 44-Control Template at 37 °C

substrate	burst rate (s^{-1})	burst amplitude (%)	$K_{d,DNA}$ (nM) (polymerase site)
22/44-mer	41 ± 2	97 ± 2	8 ± 2
23/44-mer	26 ± 1	89 ± 1	7 ± 2
24/44-mer	18 ± 1	82 ± 1	8 ± 3
25/44-mer	21 ± 1	98 ± 2	6 ± 2
26/44-mer	27 ± 2	51 ± 2	9 ± 3
27/44-mer	39 ± 3	43 ± 1	8 ± 3
30/44-mer	36 ± 2	56 ± 1	9 ± 2

In contrast, the time courses of product formation at pause sites with the 44-cisplatin template exhibited low burst amplitudes (1−3%) followed by a second phase at moderate rates (0.7−1.4 s^{-1}) (data not shown). To determine whether the slow phase was due to release of the DNA from the enzyme, we measured the dissociation rate of 25/44-cisplatin directly as described previously (*19*, *29*). A preincubated solution of 200 nM RT and 200 nM 5′-labeled 25/44-cisplatin·Mg^{2+} was mixed with 10 μM of unlabeled 25/45-mer·Mg^{2+} for 0.1−50 s and then mixed with 100 μM dATP and 10 mM Mg^{2+} for 10 s. The reactions were quenched with 0.3 M EDTA and analyzed on sequencing gel. The amount of labeled 26/44-cisplatin decayed by a single exponential with a rate of 0.07 s^{-1}, which is 10-fold lower than the slow-phase rate (0.73 s^{-1}) in the burst experiment. This result indicates that the slow-phase rates are not due to dissociation of DNA from enzyme at the strong pause sites. Rather, they represent a slow reaction phase occurring while the DNA remains bound to the enzyme.

Interestingly, the biphasic polymerization kinetics observed mirror the results obtained previously at the sites where HIV-1 RT paused due to RNA secondary structure effects (*29*). In the previous work we demonstrated that the biphasic polymerization observed at the pause sites was a function of two modes of binding of the DNA/RNA duplexes to RT (*29*). The small amplitude of the fast phase of polymerization is a function of a small fraction of the DNA/RNA duplexes bound productively at the polymerase site of HIV-1 RT. The remainder of the DNA/RNA duplexes are bound nonproductively initially and slowly converted to the productive mode without dissociation from the enzyme, allowing polymerization to occur (*29*).

If this mechanism also applies to the strong RT pausing caused by the *cis*-[$Pt(NH_3)_2${d(GpG)-N7(1),-N7(2)}] cross-link, incorporation of the next nucleotide to 23/44-cisplatin, 24/44-cisplatin, or 25/44-cisplatin, in a single enzyme binding event, should follow biphasic kinetics at each pause site as previously observed (*29*). To examine this hypothesis, we measured the kinetics of next nucleotide incorporation in a single turnover in the presence of an excess DNA trap to sequester free RT and prevent multiple binding events. A preincubated solution of 100 nM 5′-labeled 23/44-cisplatin, 10 mM Mg^{2+}, and 150 nM RT was mixed with a solution of 150 μM Mg^{2+}·dCTP and 5 μM unlabeled DNA 25/45-mer. Polymerization was quenched with 0.3 M EDTA at time intervals ranging from 10 ms to 75 s. The reaction products were analyzed on a sequencing gel. The resulting time course of product formation follows biphasic kinetics (Figure 4). The data were fitted to eq 2 (see Materials and Methods).

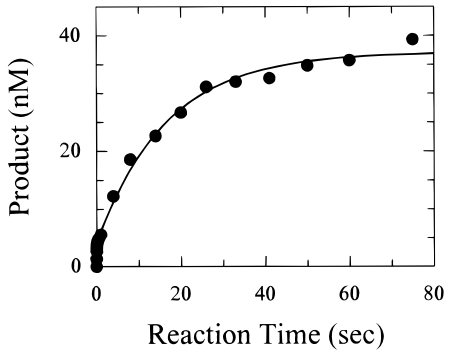

FIGURE 4: Biphasic kinetics of incorporation of dCTP into 23/44-cisplatin catalyzed by HIV-1 RT at 37 °C. A solution of RT (150 nM) was incubated with 5′ ^{32}P-labeled 23/44-cisplatin (100 nM) and then was mixed with dCTP (150 μM), unlabeled 25/45-mer (5 μM), and Mg^{2+} (10 mM). The reactions were quenched at time intervals ranging from 10 ms to 75 s by the addition of 0.3 M EDTA. DNA products were quantitated by sequencing gel analysis. The data (●) were fitted to eq 2, which gave a fast rate of 32 s^{-1} with an amplitude of 2.8% and a slow rate of 0.061 s^{-1} with an amplitude of 22%, relative to the enzyme concentration.

The fast phase occurred at a rate of 32 s^{-1} and a reaction amplitude of 2.8%, whereas the slow phase occurred with a rate of 0.061 s^{-1} and a reaction amplitude of 22% relative to the total RT concentration.

Similar experiments were performed with 24/44-cisplatin and 25/44-cisplatin, and the results are listed in Table 2. The reaction amplitudes of the fast phase at the three pause sites are small (1 to 3%). The slow-phase reaction amplitudes of 23/44-cisplatin and 25/44-cisplatin are significantly larger than that of 24/44-cisplatin. The observation of biphasic kinetics of next nucleotide incorporation at the three pause sites in the presence of DNA trap indicates that 23/44-cisplatin, 24/44-cisplatin, and 25/44-cisplatin bind to HIV-1 RT in both productive and nonproductive modes, with the conversion from nonproductive to productive binding limiting the rate of the slow phase.

When similar experiments were performed with primers positioned after the adduct (26/44-cisplatin, 26/44-control) or before the adduct (22/44-cisplatin), we observed only the fast phase of polymerization (data not shown). The time courses of product formation were fitted to eq 3, and the resulting fast rates and reaction amplitudes agree with those obtained from the burst experiments (Table 2). These results demonstrate that the mechanisms of nucleotide incorporation catalyzed by HIV-1 RT at pause and nonpause sites are different.

To test whether the above mechanistic reasoning also applies to the stalling of T7 exo$^-$ owing to the *cis*-[$Pt(NH_3)_2$-{d(GpG)-N7(1),-N7(2)}] cross-link, we performed similar burst experiments at nonpause sites with the 44-cisplatin and 44-control templates. The results are listed in Tables 4 and 5. The burst rates, steady-state rates, and burst amplitudes vary with the sizes of primers. With the 44-control template, the burst amplitude increases and the steady-state rate decreases when the size of the primer increases. The minimum-sized primer of 25 nucleotides is required to reach full burst amplitude and a slower than 0.1 s^{-1} steady-state rate (Table 5). With the 44-cisplatin template, the burst rates are significantly lower with the primers, ranging from the 27- to 30-mer than with other primers. This result agrees with the observation of slight accumulation of intermediates

Table 4: Kinetic Constants and Binding Affinity of T7 DNA Polymerase and DNA Substrates with the 44-Cisplatin Template at 20 °C[a]

substrate	fast rate (s^{-1})	amplitude (fast phase) (%)	slow rate (s^{-1})	amplitude (slow phase) (%)	$K_{d,DNA}$ (nM) polymerase site	$K_{d,dNTP}$ (μM)
22/44-mer	33 ± 2	57 ± 4			31 ± 5	61 ± 11
23/44-mer	53 ± 7	1.8 ± 0.1	0.06 ± 0.02	0.8 ± 0.1		
24/44-mer	161 ± 21	2.3 ± 0.1	0.06 ± 0.03	0.7 ± 0.1		
25/44-mer	199 ± 36	1.6 ± 0.1	0.04 ± 0.01	3.0 ± 0.2		
26/44-mer	31 ± 2	55 ± 5			115 ± 9	85 ± 18
27/44-mer	2 ± 1	74 ± 7			52 ± 4	252 ± 55
28/44-mer	3 ± 1	83 ± 5				
29/44-mer	9 ± 3	86 ± 6			24 ± 7	12 ± 4
30/44-mer	7 ± 3	90 ± 6				
31/44-mer	60 ± 23	88 ± 5				
32/44-mer	153 ± 36	91 ± 6			12 ± 1	9 ± 1

[a] The substrates corresponding to the strong pause sites are in boldface.

Table 5: Kinetic Constants and Binding Affinity of T7 DNA Polymerase and DNA Substrates with the 44-Control Template at 20 °C

substrate	burst rate (s^{-1})	burst amplitude (%)	steady-state rate (s^{-1})
22/44-mer	50 ± 11	37 ± 2	0.51 ± 0.05
23/44-mer	48 ± 11	54 ± 4	0.26 ± 0.04
24/44-mer	182 ± 37	71 ± 2	0.16 ± 0.02
25/44-mer	194 ± 17	96 ± 2	0.09 ± 0.01
26/44-mer	83 ± 10	98 ± 4	0.03 ± 0.02
27/44-mer	95 ± 7	98 ± 2	0.05 ± 0.01
30/44-mer	114 ± 16	97 ± 3	0.07 ± 0.02

27-, 28-, 29-, and 30-mer during the processive polymerization on 26/44-cisplatin (data not shown).

At strong pause sites, we measured the kinetics of single nucleotide incorporation into 23/44-cisplatin, or 24/44-cisplatin, or 25/44-cisplatin catalyzed by T7 exo$^-$, in a single turnover experiment in the presence of an excess DNA trap 25/45-mer. The kinetics (not shown) were biphasic, as described above for HIV-1 RT (see Figure 4); fitting the data to a double exponential yielded the results summarized in Table 4. Although the amplitudes of both phases are small, the biphasic kinetics of next nucleotide incorporation indicates that cisplatin-modified DNA binds to T7 exo$^-$ in both productive and nonproductive modes at pause sites.

As shown in Tables 2 and 4, the reaction amplitudes of the fast phase are much lower at pause sites than at nonpause sites. This result suggests that the binding of DNA substrates to RT or T7 exo$^-$ is affected by the *cis*-[Pt(NH$_3$)$_2$\{d(GpG)-N7(1),-N7(2)\}] cross-link. To verify this conclusion, we measured the binding affinity of DNA by two different methods: active-site titration and nitrocellulose-DEAE double filter binding assay.

Measurement of the Affinity of DNA by Active-Site Titration. The reaction amplitude of the fast phase corresponds to the percentage of enzyme that initially binds DNA productively in the preequilibrated solution of enzyme and DNA. The active-site titration was performed by incubating a fixed concentration of 60 nM RT with increasing concentrations of 5′ ^{32}P-labeled 26/44-cisplatin at 37 °C. The amount of active RT·DNA complex present in solution was then measured by rapidly mixing it with a solution of 200 μM Mg^{2+}·dGTP (concentrations before mixing) to allow a single turnover. Reactions were then quenched after seven half-times (162 ms), which allowed adequate time to reach the maximum burst amplitude in the fast phase with negligible contribution from multiple turnovers or the slow reaction phase, thus affording a direct measurement of the concentration of productive E·DNA complexes. The dependence of the enzyme reaction amplitudes on the 26/44-cisplatin concentration (before mixing) is shown in Figure 5A (active-site titration). The solid line is a fit of the data to eq 5, which gives a K_d for the RT·26/44-cisplatin complex of 17 ± 2 nM.

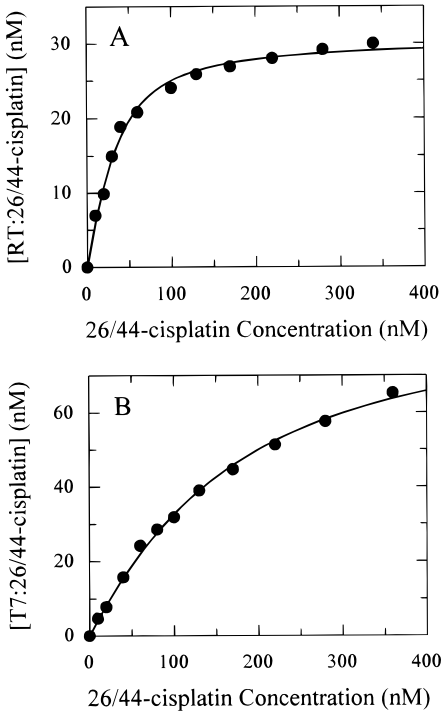

FIGURE 5: Active-site titration of HIV-1 RT and T7 exo$^-$ with the 26/44-cisplatin. (A) RT (60 nM) and Mg^{2+} (10 mM) were incubated with increasing concentrations of 5′ ^{32}P-labeled 26/44-cisplatin and then mixed with a solution of dGTP (200 μM) and Mg^{2+} (10 mM) (before mixing concentrations) at 37 °C. The reactions were quenched after 162 ms by 0.3 M EDTA. The data represent the burst amplitudes at the respective 26/44-cisplatin concentrations (before mixing). The solid line is a fit of the data (●) to eq 5, which gave a K_d value for the RT·26/44-cisplatin complex of 17 ± 2 nM, and an amplitude of 51 ± 1%. (B) T7 exo$^-$ (150 nM), *E. coli* thioredoxin (2.4 μM), and DTT (10 mM) were incubated with increasing concentrations of 5′ ^{32}P-labeled 26/44-cisplatin and then mixed with a solution of dGTP (100 μM) and Mg^{2+} (12.5 mM) in T7 buffer at 20 °C. The reactions were terminated after 157 ms by 0.3 M EDTA. The data (●) were fitted to eq 5, which gave a K_d value for the T7 exo$^-$·26/44-cisplatin complex of 115 ± 9 nM and an amplitude of (59 ± 2)%.

The same active site titration was conducted at other sites with the 44-cisplatin and 44-control templates, and the results

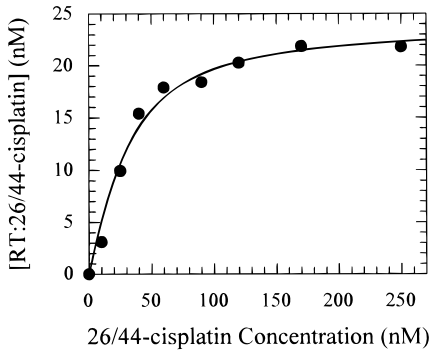

FIGURE 6: Overall binding affinity of the 26/44-cisplatin to HIV-1 RT at 23 °C. The K_d for formation of the RT·26/44-cisplatin complex was measured using a nitrocellulose−DEAE membrane filter binding assay. RT (45 nM) and Mg^{2+} (10 mM) were incubated with increasing concentrations of 5′ ^{32}P-labeled 26/44-cisplatin and then applied to the wells of a nitrocellulose and DEAE double-filter dot-blot apparatus. The solid line is a fit of the data (●) to eq 5, which gave a K_d value for the RT·26/44-cisplatin complex of 18 ± 4 nM and an amplitude of 54 ± 2%.

are summarized in Table 2. These results clearly show that DNA substrates are bound tightly to RT at nonpause sites with the 44-cisplatin template and at all sites with the 44-control template. In contrast, the binding of DNA to the polymerase site of RT at the three pause sites appears weaker. The K_d values at the pause sites have large error ranges due to the inaccuracy of measuring the small reaction amplitudes of the fast phase and the higher apparent K_d.

A similar active-site titration was performed with T7 exo$^-$ and 26/44-cisplatin at 20 °C. The binding affinity of 26/44-cisplatin to T7 exo$^-$ was estimated to be 115 ± 2 nM (Figure 5B). By using the same method, we also measured the affinity of four other DNA substrates with the 44-cisplatin template to the polymerase site of T7 exo$^-$ (Table 4).

Measurement of Overall Affinity of DNA to HIV-1 RT by Nitrocellulose−DEAE Double-Filter Binding Assay at 23 °C. At the three pause sites, the kinetic analyses have shown that only a small percentage of HIV-1 RT binds DNA in a productive mode and most of the enzyme molecules bind DNA in a nonproductive mode. The nonproductively bound DNA remains associated with RT during the slow phase of the reaction and is converted to product or dissociates slowly from enzyme. Because the active-site titration cannot measure the binding affinity of DNA substrates at the three pause sites accurately (Table 2) and because the active-site titration measures only DNA binding in the productive mode, it was necessary to use a method that measures total DNA binding to the enzyme with higher accuracy, but which can assess the same affinity (*29*). We therefore measured the overall binding of DNA to RT by using nitrocellulose−DEAE double-filter binding assay (see Materials and Methods). After allowing equilibration of 45 nM RT and 10 mM Mg^{2+} with increasing concentrations of 5′-labeled 36/66-mer, the samples were applied to the double filters. After washing with RT buffer, the nitrocellulose membrane retains the RT·26/44-cisplatin complex and the DEAE membrane traps all remaining 26/44-cisplatin duplexes. Figure 6 plots the average concentrations of the RT·26/44-cisplatin complex retained by the nitrocellulose membrane, after correction for nonspecific retention of free DNA, against the total concentration of the 26/44-cisplatin duplexes. The data were fitted to eq 5, which gave a K_d for the RT·26/44-cisplatin complex of 18 ± 4 nM. Thus, both methods of measuring binding affinity provided the same value.

The same double-filter assay was used to measure the overall binding affinity of DNA to RT using other primer lengths with the 44-cisplatin template. The data are summarized in Table 2. The overall binding affinity of all DNA substrates to RT is high, suggesting that the cisplatin adduct does not significantly alter the affinity of DNA to the binding cleft of RT. At each strong pause site, the K_d value for total DNA binding measured by the double-filter assay is significantly smaller than the K_d for binding to the polymerase site of RT measured by the active-site titration. It is not clear why the difference is so large. This discrepancy is most probably due to the inaccuracies in measuring the small reaction amplitudes in the fast phase (1−3%) (*29*) since the two methods should provide the same parameter (*29*).

We also tried to use the double-filter binding assay to measure the overall binding affinity of DNA to T7 exo$^-$ and observed a small degree of retention of the 5′ ^{32}P-labeled DNA to the nitrocellulose membrane. This result may be because the T7 exo$^-$·DNA complexes are too-short-lived to be retained by the nitrocellulose membrane (*25*).

Measurement of Ground-State Binding Affinity of Next Correct Nucleotide to the T7 exo$^-$·DNA Complex. Ground-state nucleotide binding involves proper base pairing to the DNA template (*18*). The base pairs are propeller twisted around the *cis*-[Pt(NH$_3$)$_2$\{d(GpG)-N7(1),-N7(2)\}] cross-link on the basis of both X-ray crystal (*9*, *10*) and NMR structural data (*11*−*13*). Thus, the ground-state nucleotide binding could have been affected by the cisplatin−DNA cross-link. To examine this possibility, we measured the ground-state affinity of the next correct nucleotide to the T7 exo$^-$·DNA complexes by reacting a preincubated solution of T7 exo$^-$ and the primer/44-cisplatin duplexes with varying concentrations of Mg^{2+}·dNTP and monitoring product formation with time. As shown in Figure 7A, the single-turnover rates for formation of 27/44-cisplatin product increase with increasing concentrations of dGTP. The dependence of the burst rate on the dGTP concentration is shown in Figure 7B along with the fit to eq 4 that afforded a K_d of 85 ± 18 μM and a maximum rate of incorporation of 35 ± 3 s^{-1}. This K_d value is nearly 20-fold weaker than previously measured (*26*).

Similar experiments were performed to assess the ground-state affinity of next nucleotides with the 22/44-cisplatin, 27/44-cisplatin, 29/44-cisplatin, and 32/44-cisplatin duplexes, and the results are summarized in Table 4. The values of the ground-state nucleotide binding affinity indicate that the *cis*-[Pt(NH$_3$)$_2$\{d(GpG)-N7(1),-N7(2)\}] cross-link on the template affects the binding of the next nucleotide to the T7 exo$^-$·DNA binary complexes.

DISCUSSION

Differential Processive Polymerization on 19/44-Cisplatin Catalyzed by HIV-1 RT and T7 DNA Polymerase. The intermediate accumulation patterns during processive polymerization (Figures 2A and 3A) clearly reveal that the cisplatin adduct significantly blocked polymerization. Both HIV-1 RT and T7 exo$^-$ strongly paused one nucleotide prior to the first platinated guanine (nucleotides 23 from the template 3′ terminus) and at the two platinated guanines (nucleotide 24 and 25). The stalling of T7 exo$^-$ in Figure

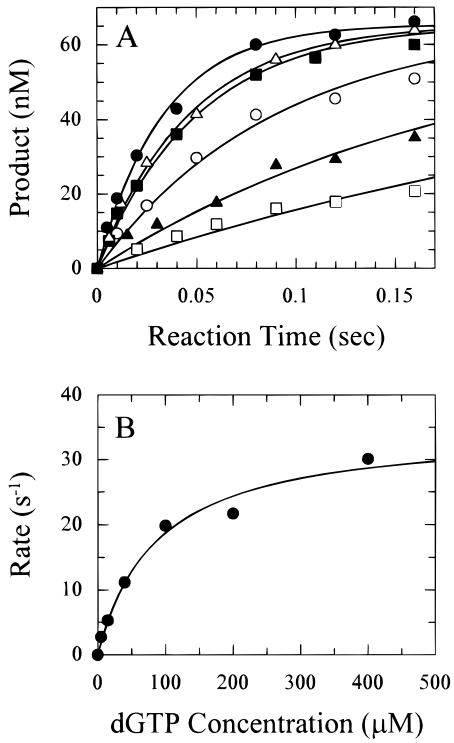

FIGURE 7: dGTP concentration dependence on the pre-steady-state burst rate at 20 °C with T7 exo⁻ and the 26/44-cisplatin. (A) A preincubated solution of T7 exo⁻ (120 nM), *E. coli* thioredoxin (2.4 μM), 5′ ^{32}P-labeled 26/44-cisplatin (200 nM), and DTT (10 mM) was mixed with increasing concentrations of dGTP in 12.5 mM Mg^{2+} containing T7 buffer to start the reactions (final concentrations). The reactions were quenched at the indicated times and analyzed by sequencing gel electrophoresis. The dGTP concentrations were 5 (□), 15 (▲), 40 (○), 100 (■), 200 (△), and 400 μM (●). The solid lines represent the best fit of data to eq 3. (B) The first-order rates (●) measured from the time courses in the above experiments were plotted against the dGTP concentrations. The fit to eq 4 (solid line) yielded a K_d value of 85 ± 18 μM for dGTP dissociation and a maximum rate of incorporation of 35 ± 3 s^{-1}.

3A agrees with a previous report of polymerization inhibition by a single *cis*-[Pt(NH_3)$_2$\{d(GpG)-N7(1),-N7(2)\}] cross-link (*3*). Moreover, the single turnover kinetic studies reported here demonstrate that the accumulation is not just due to dissociation of the DNA from the enzyme at the site of the adduct. Rather the modified DNA remains bound to the enzyme at the pause site and slowly elongates or dissociates. The lack of accumulation of intermediates between the site opposite the adduct (25 nucleotides) and the full-length product is due to the slow rate of extension past the adduct, relative to faster extension of longer species. The observation implies only that the extension of all species beyond the adduct must be faster than their rate of formation.

The blocking of DNA synthesis catalyzed by T7 exo⁻ at the first two positions is so efficient that accumulation of the 25-mer is almost undetectable even after a 10 min reaction time, consistent with the high fidelity of T7 polymerase. HIV RT shows a much lower fidelity (1 error in 10^3−10^4) (*19*) compared to T7 DNA polymerase (10^5−10^6 in the absence of the proofreading function) (*27*). The replication bypass efficiency of HIV-T RT is higher than that of T7 exo⁻, possibly because of the lower stringency of base pairing or the requirement for polymerization catalyzed by HIV-1 RT to accommodate both RNA and DNA templates. The replication bypass efficiency of wild-type T7 DNA polymerase, or other polymerases containing the 3′-5′ proofreading exonuclease, will be even lower because of continued insertion and removal of the bases opposite the adduct, causing the polymerase to stall. In the absence of a proofreading function, forward movement is continuous although slow.

Translesion Synthesis Is Not a Consequence of Deplatination of the 44-Cisplatin Template. With the 44-cisplatin template, the translesion synthesis is not due to platinum removal based on the following reasons. First, the purity of the 44-cisplatin is >99%, as monitored by 5′-^{32}P-labeling and polyacrylamide gel electrophoresis (data not shown). Second, since the platinum adducts are stable under a variety of harsh temperature and pH conditions (*3*), the 44-cisplatin template should be able to withstand our reaction conditions. The presence of the sulfur donor ligand, 10 mM DTT, in the T7 reaction buffer may slightly increase platinum removal, but overall deplatination should remain at a very low level (<0.7%) (*3*). Finally, the small amount of unplatinated 44-mer could not account for the large quantity of the full-length product formed after long reaction times, particularly with HIV-1 RT.

DNA Bending Effect on Polymerization. The crystal structure of the HIV-1 RT·18/19-mer·Fab has a clearly delineated 40−45° DNA bend at the fourth base pair from the primer 3′-end and a change from B-type to A-type stereochemically (*14*). The bending of unmodified DNA substrates in the polymerase active site of RT may be energetically costly, and accordingly we might expect that the binding of bent cisplatin-modified DNA substrates to RT may be tighter, or the nucleotide-induced protein conformational change might be faster, or the dissociation of RT·DNA might be slower than with the 44-control template. We observed nearly identical results from the processive polymerization on 27/44-cisplatin and 27/44-control (data not shown) indicating that the cisplatin−DNA adduct did not favor the kinetics of elongation of a 27-mer. Thus, the embedded *cis*-[Pt(NH_3)$_2$\{d(GpG)-N7(1),-N7(2)\}] cross-link did not favorably alter the polymerization catalyzed by HIV-1 RT. The 44-cisplatin template may not be the best model for the bent DNA at the binding cleft of HIV-1 RT because the *cis*-[Pt(NH_3)$_2$\{d(GpG)-N7(1),-N7(2)\}] cross-link has an unfavorable close interaction with HIV-1 RT, and because the cisplatin−DNA adduct may bend the DNA duplex (78°) (*13*) more than that RT bends DNA in the RT·DNA complex (40−45°) (*14*). Given the nature of the cisplatin adduct and the importance of DNA structure at positions three to four residues from the primer 3′-terminus, it is in some sense surprising that it has no negative effects on the polymerization kinetics at sites past the adduct.

Kinetics at Nonpause Sites with HIV-1 RT. The kinetic parameters observed with the 44-cisplatin template and primers other than 23-, 24-, and 25-mer are similar to those obtained with the corresponding substrates with the 44-control template. It is important to note, however, that the enzyme reaction amplitudes with substrates 22/44-control, 23/44-control, 24/44-control, 25/44-control, and 22/44-cisplatin are close to 100%, which are twice as great as the enzyme reaction amplitudes seen with 26-, 27-, and 30-mer primers and both templates. There is a continued debate as to the origin of the lower than 100% reaction amplitudes

observed with most preparations of HIV RT, and proposals to explain the lower amplitudes have ranged from dead enzyme to errors in the extinction coefficient used to determine protein concentration (*19*, *20*). However, these results and those of others (*20*, *22*) may imply that the different enzyme reaction amplitudes are due to DNA sequence-dependent effects and may reflect a portion of the DNA binding in a nonproductive mode. The productive mode of binding is operationally defined as a state whereby the DNA is configured to rapidly accept an incoming nucleotide. A fraction of the DNA binding in a mode that leads to dissociation of the DNA from the enzyme at a rate faster than elongation would be defined as nonproductive and would lead to a reduced burst amplitude. Subtle changes in DNA structure and its positioning in the active site could lead to what we observe as nonproductive binding.

Optimal DNA Binding Size to T7 DNA Polymerase. The kinetics of nucleotide incorporation catalyzed by T7 exo$^-$ at all sites with the 44-control template is consistent with previous work (*26*). The burst amplitude increases from 37% to 96%, and the steady-state rate decreases from 0.5 to 0.1 s^{-1} as the length of primer increases from 22 to 25 nucleotides (Table 5). When the primer is longer than 25 nucleotides, the enzyme reaction amplitude remains close to 100% and the steady-state rate is below 0.1 s^{-1}. These results suggest an optimal DNA binding size of 25 base pairs, which is larger than the size of 21 base pairs of duplex DNA protected by T7 DNA polymerase and *E. coli* thioredoxin detected by exonuclease degradation in footprint analysis (*35*). Pre-steady-state kinetic analysis provides an assessment of the optimal DNA binding size required for function, since it measures only the productive binding at the enzyme active site.

Kinetics at Nonpause and Weak Pause Sites with T7 DNA Polymerase. The kinetics observed with the 44-cisplatin template and T7 exo$^-$ is more complex than that for HIV-1 RT. For example, a significantly higher burst amplitude was observed with 22/44-cisplatin (57%) than with 22/44-control (37%). The crystal structure of the T7 DNA polymerase·DNA·ddGTP complex has revealed that the template strand enters the polymerase active site from the side facing away from the thumb, and a sharp turn exposes the template base for interaction with the incoming nucleotide (*15*). Thus, the higher burst amplitudes with primers shorter than 23-mer are possibly due to the *cis*-[Pt(NH$_3$)$_2$\{d(GpG)-N7(1),-N7(2)\}] cross-link, which will bend the single-stranded 5′-end of template by 75−82° (*36*) and facilitate binding of DNA to the T7 DNA polymerase.

With the primers extending beyond the second platinated guanine, we expect that the polymerization catalyzed by T7 exo$^-$ should return to normal as observed with HIV-1 RT. But Table 4 reveals that the inhibitory effect of the *cis*-[Pt(NH$_3$)$_2$\{d(GpG)-N7(1),-N7(2)\}] cross-link on the kinetics of DNA synthesis does not diminish until the primer is longer than 30 nucleotides. With 27- to 30-nucleotide primers, the burst rates (2−9 s^{-1}) are significantly lower and the binding of DNA substrates and next nucleotides is also weaker than those of the 32/44-cisplatin, accounting for the slight accumulation of the 27- to 30-mer intermediates during processive polymerization. The much lower burst rates suggest that the rate-limiting protein conformational change has been inhibited by the embedded *cis*-[Pt(NH$_3$)$_2$\{d(GpG)-N7(1),-N7(2)\}] cross-link, an effect extending five nucleotides into the DNA substrate.

Kinetics at the Three Strong Pause Sites. Both HIV-1 RT and T7 exo$^-$ stalled after synthesis of the 23-, 24-, and 25-mer with the 44-cisplatin template and showed biphasic kinetics at each pause site. Only a small fraction of the HIV-1 RT·DNA or T7 exo$^-$·DNA complex was able to catalyze DNA synthesis rapidly, while the remainder of the DNA was bound in a nonproductive mode. Interestingly, a similar effect has been observed at the strong HIV-1 RT pause sites attributed to RNA secondary structure effects (*29*). At pause sites while the polymerase was encountering RNA template secondary structure, analysis of the RNase H activity provided additional evidence to suggest that the template was shifted out of the polymerase site by two to three residues in the nonproductive binding mode at the pause sites. The nature of the nonproductive binding mode with the cisplatin adduct is not known, but it may represent a similar misplacement of the primer 3′-OH out of the active site necessary for continued polymerization. The total reaction amplitude summing the fast and slow phases with the 44-cisplatin template is still less than that of the corresponding control DNA substrate, which suggests that some of the nonproductively bound primer/44-cisplatin may have dissociated from the enzyme before being elongated or that its elongation was not observed in the time domain we used.

Our kinetic data generally show effects that correlate with the twisted angles of base pairs around the cisplatin−DNA adduct predicted by the crystal structure of cisplatin-modified dodecamer duplex (*9*, *10*), although a strict correlation would have predicted a greater accumulation of the 22-mer than we observed. Nonetheless, the correlation suggests that twisting of the base pair in the DNA structure is responsible for the pausing.

Tight Binding of the Primer/44-Cisplatin to HIV-1 RT. HIV-1 RT binds tightly to each DNA substrate investigated. The enzyme has a binding cleft larger than 19 base pairs on the basis of crystal structure (*14*, *24*) and footprint data (*37*). Since HIV-1 RT binds DNA substrates tightly even in the presence of template secondary structure (*29*), we anticipated that HIV-1 RT would tightly bind the primer/44-cisplatin duplexes. This expectation was confirmed by the high overall binding affinity (10−20 nM) of all tested substrates (Table 2). These results indicate that the *cis*-[Pt(NH$_3$)$_2$\{d(GpG)-N7(1),-N7(2)\}] cross-link does not affect the overall tight binding of DNA to HIV-1 RT, although it has a dramatic effect on the productive DNA binding at the polymerase site of RT.

Binding of the Primer/44-Cisplatin to T7 DNA Polymerase. The binding affinity of several platinated DNA substrates to T7 exo$^-$ was measured by the active-site titration method. The closer the primer 3′-end is to the platinated guanines, the weaker the DNA binding. Although we could not determine the binding affinity of 23/44-cisplatin, 24/44-cisplatin, and 25/44-cisplatin to T7 exo$^-$ due to very small reaction amplitudes in the fast phase, the slightly different binding affinities of the five tested substrates suggest that T7 DNA polymerase is more sensitive to DNA structure changes induced by the cisplatin−DNA adduct than is HIV-1 RT. This finding is consistent with the ability of HIV-1 RT to accept both RNA and DNA templates.

Scheme 1

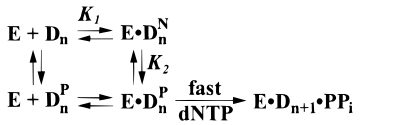

Binding of Next Correct Nucleotide to the T7 exo⁻·Primer/44-Cisplatin Complex. The binding affinity of the next correct nucleotide to the E·DNA complex to form the productive ground-state E·DNA·dNTP complex is determined by proper base pairing with the DNA template (*18*). Although not directly measured, the ground-state binding affinity of the next nucleotide to HIV-1 RT does not seem to be affected at nonpause sites by the cisplatin−DNA adduct because the kinetics of next nucleotide incorporation with the 44-cisplatin template is very similar to that with the unplatinated 44-control template. A weaker affinity would have led to a slower observed rate. With T7 exo⁻, however, the binding affinity of next nucleotide was affected by the cisplatin−DNA adduct. The closer the next base pair from the adduct, the weaker the ground-state binding of the next nucleotide. This result provides additional evidence that T7 DNA polymerase has a more stringent geometric requirement for base pairing at the polymerase active site than HIV-1 RT.

The cisplatin−DNA modification sites are mutational hot spots (*3*). In a study of the *cis*-[Pt(NH$_3$)$_2$\{d(ApG)-N7(1),-N7(2)\}] cross-link, a mutational frequency of 1−2% was scored and these adducts were five times more mutagenic than *cis*-[Pt(NH$_3$)$_2$\{d(GpG)-N7(1),-N7(2)\}] cross-links (*38*). When we carried out the processive polymerization with the 44-cisplatin template and wild-type HIV-1 RT, more 23-, 24-, and 25-mer accumulated in the presence of, rather than in the absence of, nucleotide analogues dideoxycytidine triphosphate and 9-(2-(phosphonylmethoxy)propyl)adenine diphosphate (data not shown). This result indicates that the inhibition of HIV-1 RT by the cisplatin−DNA adduct and nucleotide analogues has more than additive effects.

Although one cisplatin−DNA adduct cannot completely inhibit replication, the HIV RNA genome has over 9000 nucleotides, and HIV RT catalyzes incorporation of over 20 000 nucleotides during one viral life cycle. Platinum-based antitumor drugs including cisplatin will form numerous covalent adducts with bases of both DNA and RNA per virus if absorbed by HIV. The platinum antitumor drugs alone could inhibit HIV reverse transcription completely. The inhibition could be more effective if the platinum antitumor drugs were used in combination with nucleoside inhibitors.

Universal Mechanism of Polymerase Pausing. The mechanism of pausing due to RNA (*29*) and DNA (*39*) secondary structure effect has been previously described and is illustrated in Scheme 1. A small percentage of DNA molecules bound productively at the polymerase site of enzyme (E·D_nP) rapidly accept the next nucleotide to form the elongated product. This reaction occurs in the fast phase. Other DNA molecules are bound nonproductively (E·D_nN), slowly convert to the productively bound state, and are then converted to products. The slow conversion of the DNA from the nonproductive to the productive state, without dissociation from the enzyme, accounts for the slow reaction phase. The observed biphasic kinetics of nucleotide incorporation catalyzed by both HIV-1 RT and T7 DNA polymerase at the three strong pause sites due to the *cis*-[Pt(NH$_3$)$_2$\{d(GpG)-N7(1),-N7(2)\}] cross-link can be explained by such a mechanism, and it should apply to other types of intrastrand cisplatin−DNA adducts or other adducts as well.

The structure of the nonproductive complex (E·D_nN) with the 44-cisplatin template is not known. The location of the primer 3′-OH may not be well-positioned in the active site for catalysis because of propeller twisting by the cisplatin−DNA adduct. For the conversion of the nonproductive bound state to the productive state, the 3′-OH of the sugar has to be in line to attack the α-phosphate of an incoming nucleoside triphosphate. The required geometry could involve changes in structure of the enzyme, the DNA, or both.

ACKNOWLEDGMENT

The authors thank Allison Johnson (The Pennsylvania State University) for purifying the exonuclease-deficient T7 DNA polymerase, Dr. Andrew Gelasco (Massachusetts Institute of Technology) for purifying the 12 nucleotide DNA containing a single *cis*-[Pt(NH$_3$)$_2$\{d(GpG)-N7(1),-N7(2)\}] cross-link, and Dr. Roger Goody (Max-Planck Institute, Heidelberg) for providing the clone of wild-type HIV-1 RT (p66/p51).

REFERENCES

1. Sherman, S. E., and Lippard, S. J. (1987) *Chem. Rev. 87*, 1153−1181.
2. Abrams, M. J., and Murrer, B. A. (1993) *Science 261*, 725−730.
3. Comess, K. M., Burstyn, J. N., Essigmann, J. M., and Lippard, S. J. (1992) *Biochemistry 31*, 3975−3990.
4. Reedijk, J. (1987) *Pure Appl. Chem. 59*, 181−192.
5. Lippard, S. J. (1987) *Pure Appl. Chem. 59*, 731−742.
6. Corda, Y., Job, C., Anin, M. F., Leng, M., and Job, D. (1991) *Biochemistry 30*, 222−230.
7. Page, J. D., Husain, I., Sancar, A., and Chaney, S. G. (1990) *Biochemistry 29*, 1016−1024.
8. Zamble, D. B., and Lippard, S. J. (1995) *Trends Biochem. Sci. 20*, 435−439.
9. Takahara, P. M., Rosenzweig, A. C., Frederick, C. A., and Lippard, S. J. (1995) *Nature 377*, 649−652.
10. Takahara, P. M., Frederick, C. A., and Lippard S. J. (1996) *J. Am. Chem. Soc. 118*, 12309−12321.
11. Yang, D., van Boom, S. S. G. E., Reedijk, J., van Boom, J. H., and Wang, A. H.-J. (1995) *Biochemistry 34*, 12912−12920.
12. Dunham, S. U., Dunham, S., Turner, C. J., and Lippard, S. J. (1998) *J. Am. Chem. Soc. 120*, 5395−5406.
13. Gelasco, A. K., and Lippard, S. J. (1998) *Biochemistry 37*, 9230−9239.
14. Jacobo-Molina, A., Ding, J., Nanni, R. G., Clark, A. D., Jr., Lu, X., Tantillo, C., Williams, R. L., Kamer, G., Ferris, A. L., Clark, P., Hizi, A., Hughes, S. H., and Arnold, E. (1993) *Proc. Natl. Acad. Sci. U.S.A. 90*, 6320−6324.
15. Doublie, S., Tabor, S., Long, A. M., Richardson, C. C., and Ellenberger, T. (1998) *Nature 391*, 251−258.
16. Hoffman, A. D., Banapour, B., and Levy, J. A. (1985) *Virology 147*, 326−335.
17. Goff, S. (1990) *J. AIDS 3*, 817−819.
18. Johnson, K. A. (1993) *Annu. Rev. Biochem. 62*, 685−713.
19. Kati, W. M., Johnson, K. A., Jerva, L. F., and Anderson, K. S. (1992) *J. Biol. Chem. 267*, 25988−25997.
20. Reardon, J. E. (1992) *Biochemistry 31*, 4473−4479.
21. Reardon, J. E. (1993) *J. Biol. Chem. 268*, 8743−8751.
22. Hsieh, J. C., Zinnen, S., and Modrich, P. (1993) *J. Biol. Chem. 268*, 24607−24613.

23. Rodgers, D. W., Gamblin, S. J., Harris, B. A., Ray, S., Culp, J. S., Hellmig, B., Woolf, D. J., Debouck, C., and Harrison, S. C. (1995) *Proc. Natl. Acad. Sci. U.S.A. 92*, 1222−1226.
24. Kohlstaedt, L. A., Wang, J., Friedman, J. M., Rice, P. A., and Steitz, T. A. (1992) *Science 256*, 1783−1790.
25. Huber, H. E., Tabor, S., and Richardson, C. C. (1987) *J. Biol. Chem. 262*, 16224−16232.
26. Patel, S. S., Wong, I., and Johnson, K. A. (1991) *Biochemistry 30*, 511−525.
27. Wong, I., Patel, S. S., and Johnson, K. A. (1991) *Biochemistry 30*, 526−537.
28. Donlin, M. J., Patel, S. S., and Johnson, K. A. (1991) *Biochemistry 30*, 538−546.
29. Suo, Z., and Johnson, K. A. (1997) *Biochemistry 36*, 12459−12467.
30. Bellon, S. F., and Lippard, S. J. (1990) *Biophys. Chem. 35*, 179−188.
31. Dawson, R. M. C., Elliott, D. C., Elliott, W. H., and Jones, K. M. (1987) *Data for Biochemical Research*, Oxford University Press, New York.
32. Johnson, K. A. (1986) *Methods Enzymol. 134*, 677−705.
33. Wong, I., and Lohman, T. M. (1993) *Proc. Natl. Acad. Sci. U.S.A. 90*, 5428−5432.
34. Leis, J., Aiyar, A., and Cobrinik, D. (1993) in *Reverse Transcriptase* (Skalka, A. M. and Goff, S. P., Eds.) pp 33−83, Cold Spring Harbor Laboratory Press, Plainview, NY.
35. Bedford, E., Tabor, S., and Richardson, C. C. (1997) *Proc. Natl. Acad. Sci. U.S.A. 94*, 479−484.
36. Sherman, S. E., Gibson, D., Wang, A. H. J., and Lippard, S. J. (1988) *J. Am. Chem. Soc. 110*, 7368−7381.
37. Wöhrl, B. M., Tantillo, C., Arnold, E., and Le Grice, S. F. J. (1995) *Biochemistry 34*, 5343−5350.
38. Burnouf, D., Gauthier, C., Chottard, J. C., and Fuchs, R. P. P. (1990) *Proc. Natl. Acad. Sci. U.S.A. 87*, 6087−6091.
39. Suo, Z., and Johnson, K. A. (1998) *J. Biol. Chem. 273*, 27259−27267.

BI981854N